Pramana – J. Phys. (2022) 96:119
https://doi.org/10.1007/s12043-022-02357-4

Study of anisotropic compact stars in $f(\mathcal{R}, \mathcal{T}, \mathcal{R}_{\chi\xi}\mathcal{T}^{\chi\xi})$ gravity

M SHARIF* and T NASEER

Department of Mathematics, University of the Punjab, Quaid-i-Azam Campus, Lahore 54590, Pakistan
*Corresponding author. E-mail: msharif.math@pu.edu.pk

MS received 4 October 2021; revised 25 January 2022; accepted 1 February 2022

Abstract. This paper aims to examine the composition of various spherically symmetric star models which are coupled with anisotropic configuration in $f(\mathcal{R}, \mathcal{T}, \mathcal{Q})$ gravity, where $\mathcal{Q} = \mathcal{R}_{\chi\xi}\mathcal{T}^{\chi\xi}$. We discuss the physical features of compact objects by employing bag model equation of state and construct the modified field equations in terms of Krori–Barua ansatz involving the unknowns (A, B, C). The observational data of 4U 1820-30, Vela X-I, SAX J 1808.4-3658, RXJ 1856-37 and Her X-I are used to calculate these unknowns and bag constant $\mathfrak{B}_c$. Further, we observe the behaviour of energy density, radial and tangential pressure as well as anisotropy through graphical interpretation for a viable model $\mathcal{R} + \varrho\mathcal{Q}$ of this gravity. For a particular value of the coupling constant ϱ, we study the behaviour of mass, compactness, red-shift and the energy bounds. The stability of the considered stars is also checked by using two criteria. We conclude that our structure developed in this gravity is in good agreement with all the physical requirements.

Keywords. $f(\mathcal{R}, \mathcal{T}, \mathcal{R}_{\chi\xi}\mathcal{T}^{\chi\xi})$ gravity; anisotropy; compact stars.

PACS Nos **04.20.Jb; 98.80.Jk; 03.50.De**

1. Introduction

General relativity (GR) has accomplished remarkable results in resolving numerous hidden ingredients of the Universe. However, it is not satisfactory enough to scrutinise the cosmos at large scale. Many other alternate theories are therefore established to tackle the challenging mysteries such as dark matter and cosmic-accelerated expansion. Such expansion guarantees the existence of an obscure form of force with large negative pressure, known as dark energy. Thus, the modified gravitational theories have been extremely significant to unveil the enigmatic features of our Universe. The first ever modification to GR is $f(\mathcal{R})$ theory which involves higher-order curvature terms due to the insertion of generic function of the Ricci scalar instead of $\mathcal{R}$ in an Einstein–Hilbert action. The physical feasibility of different stellar structures has been discussed by utilising multiple techniques in this theory [1–3]. Capozziello *et al* [4] studied various mathematical models and analysed their stability using the Lané–Emden equation in $f(\mathcal{R})$ theory. Numerous studies [5–9] have been done in this context to investigate the composition and evolution of astrophysical bodies.

The notion of matter–geometry coupling was initially presented by Bertolami *et al* [10] to explore more interesting features of our Universe. They considered the matter Lagrangian as a function of $\mathcal{R}$ and $\mathcal{L}_m$ to study the influence of coupling on stellar objects in $f(\mathcal{R})$ gravity. Such interaction between geometry and matter distribution encouraged many researchers to focus on the universal accelerating expansion. Recently, different modified theories have been proposed which interlinked the matter and geometry of massive structures at the action level. Harko *et al* [11] extended the $f(\mathcal{R})$ theory to $f(\mathcal{R}, \mathcal{T})$ in which $\mathcal{T}$ indicates the trace of the energy–momentum tensor (EMT). Note that the dependence from $\mathcal{T}$ may be induced by exotic imperfect fluids or quantum effects. Since in the present model, the covariant divergence of the EMT is non-zero, the motion of massive test particles is non-geodesic and an extra force, orthogonal to the four-velocity, is always present due to the coupling between matter and geometry. This force also helps to elucidate the galactic rotation curves. The fascinating results provided by this theory have prompted numerous scientists to study the astrophysical structures [12–16]. Soon after this, Haghani *et al* [17] proposed the extension of $f(\mathcal{R}, \mathcal{T})$ gravity by considering a more complicated functional of the form

Published online: 23 June 2022

$f(\mathcal{R}, \mathcal{T}, \mathcal{Q})$ in which the factor $\mathcal{Q} \equiv \mathcal{R}_{\chi\xi}\mathcal{T}^{\chi\xi}$ guarantees the presence of strong non-minimal coupling even in the case of traceless EMT. They also analysed the impact of the term $\mathcal{Q}$ on the feasibility of various models and concluded that the Lagrange multiplier approach provides conserved equations of motion in this theory. Sharif and Zubair considered two particular models in this scenario and calculated their energy bounds as well as the conditions for Dolgov–Kawasaki instability [18]. They also studied the black hole laws of thermodynamics with different choices of the matter Lagrangian [19].

Odintsov and Sáez-Gómez [20] calculated the solution of complex field equations for various models through numerical methods in $f(\mathcal{R}, \mathcal{T}, \mathcal{Q})$ gravity and stressed some serious difficulties associated with the matter instability. Ayuso *et al* [21] studied celestial objects and adopted some scalar and vector fields to obtain stability conditions for those structures in this theory. They deduced that the matter instability must appear in the case of vector field. Baffou *et al* [22] analysed the viability of the solution of modified equations of motion through the incorporation of perturbation functions. Sharif and Waseem [23,24] have done a comprehensive analysis on the physical features of different neutron star candidates coupled with isotropic as well as anisotropic configurations in this gravity. Yousaf *et al* [25–30] found the effective structure scalars in $f(\mathcal{R}, \mathcal{T}, \mathcal{Q})$ scenario to study the evolution of spherical and cylindrical static as well as non-static structures. In this scenario, we examined some physical characteristics of charged/uncharged compact structures through gravitational decoupling [31,32].

Stars are identified as astronomical objects which play fundamental roles in the formation of galaxies in our Universe. Numerous astrophysicists concentrated on the study of their structure and evolutionary phases. The inward gravitational force induced due to the mass of a star is counterbalanced by the outward pressure which is generated as a result of nuclear reactions occurring in the core of stars. When pressure is no longer enough to resist the attractive force of gravity, a gravitational collapse occurs, resulting in the death of stellar objects due to which different celestial objects such as white dwarfs, neutron stars and black holes come into existence. The investigation of such compact stars led many astronomers to examine their diverse properties. Among these massive objects, neutron stars have attracted considerable interest owing to the composition and fascinating features of their structure. Neutrons produce degeneracy pressure which counterbalances the gravitational pull and helps to keep them in hydrostatic equilibrium. In between neutron star and black hole, there is a quark star which is highly dense consisting of up, down and strange quark matter. Many researchers [33–35] analysed the inner formation of these speculative objects.

The anisotropic configured bodies play decisive roles in the study of their structural characteristics. The interior of compact stars should possess anisotropic pressure as they encompass density much higher than nuclear density [36]. Herrera and Santos [37] examined the persuasive causes and impact of anisotropy on massive structures. Harko and Mak [38] considered a particular form of anisotropic factor and calculated interior solutions for static relativistic objects. Hossein *et al* [39] studied the effects of cosmological constant Λ on massive anisotropic structures and examined their stability. Kalam *et al* [40] analysed the validity of energy conditions and stability of different anisotropic neutron stars. Paul and Deb [41] investigated the anisotropic configured compact objects and developed physically feasible solutions.

It is anticipated that the MIT bag model equation of state (EoS) helps to express the interior configuration of quark bodies [33]. Of particular interest, the compactness of celestial structures such as 4U 1820-30, 4U 1728-34, SAX J 1808.4-3658, Her X-1, RXJ 185635-3754, PSR 0943+10, etc., cannot be explained by the neutron star EoS, while MIT bag model (strange quark matter EoS) [42] expresses their compactness successfully. The discrepancy between true and false vacuum can be calculated by using the bag constant $\mathfrak{B}_c$ appearing in the bag model EoS. The increment of these value causes the quark pressure to decrease. Several investigators [43,44] utilised the MIT bag model EoS to predict the inner fluid distribution of quarks. Demorest *et al* [45] calculated the mass of a particular quark star (PSR J1614-2230) and concluded that only the MIT bag model EoS supports such heavily objects. Rahaman *et al* [46] examined some physical characteristics of a strange star having 9.9 km radius and calculated the mass of different stars using an interpolating function. A hybrid star model has been presented by Bhar [47] through Krori–Barua ansatz and the calculated mass function was found to be compatible with the observational data. Arbañil and Malheiro [48] determined the numerical solution of the hydrostatic equilibrium condition, radial perturbation as well as MIT bag model to study the effects of anisotropy on the feasibility of compact stars. Deb *et al* [49,50] studied charged/uncharged strange stars, constructed the corresponding non-singular anisotropic solutions by employing the same EoS and checked their viability through graphical observation. Sharif and his collaborators [51–56] determined anisotropic solutions corresponding to different star candidates with the help of MIT bag model.

This paper analyses the influence of anisotropy on different quark stars in view of the Krori–Barua solution for a particular model in $f(\mathcal{R}, \mathcal{T}, \mathcal{Q})$ scenario. The paper is structured as follows. The formulation of modified field equations in terms of MIT bag model and Krori–Barua ansatz is presented in the next section. In §3, we use the junction conditions at the boundary to calculate Krori–Barua constants. The graphical behaviour of various physical features of all the considered stars is analysed in §4. Lastly, §5 provides the concluding remarks.

2. The $f(\mathcal{R}, \mathcal{T}, \mathcal{Q})$ gravity

The modification of Einstein–Hilbert action (with $\kappa = 8\pi$) involving complex analytical functional f is defined as [20]

$$S_{f(\mathcal{R},\mathcal{T},\mathcal{R}_{\chi\xi}\mathcal{T}^{\chi\xi})} = \int \sqrt{-g}\left[\frac{f(\mathcal{R}, \mathcal{T}, \mathcal{R}_{\chi\xi}\mathcal{T}^{\chi\xi})}{16\pi} + \mathcal{L}_m\right] \mathrm{d}^4x, \quad (1)$$

where $\mathcal{L}_m$ represents the Lagrangian density of fluid configuration. Corresponding to action (1), the field equations take the form as

$$\mathcal{G}_{\chi\xi} = \mathcal{T}^{(\mathrm{eff})}_{\chi\xi} = -\frac{8\pi}{\mathcal{L}_m f_{\mathcal{Q}} - f_{\mathcal{R}}}\mathcal{T}^{(m)}_{\chi\xi} + \mathcal{T}^{(\mathcal{D})}_{\chi\xi}. \quad (2)$$

The term $\mathcal{G}_{\chi\xi}$ expresses the geometric structure of the celestial bodies whereas $\mathcal{T}^{(\mathrm{eff})}_{\chi\xi}$ is identified as the EMT in $f(\mathcal{R}, \mathcal{T}, \mathcal{Q})$ gravity which involves physical variables along with modified corrections. In this scenario, the sector $\mathcal{T}^{(D)}_{\chi\xi}$ appearing due to the modified gravity has the form

$$\begin{aligned}\mathcal{T}^{(\mathcal{D})}_{\chi\xi} = -\frac{1}{\mathcal{L}_m f_{\mathcal{Q}} - f_{\mathcal{R}}}\Bigg[&\left(f_{\mathcal{T}} + \frac{1}{2}\mathcal{R}f_{\mathcal{Q}}\right)\mathcal{T}^{(m)}_{\chi\xi} \\ &+ \left\{\frac{\mathcal{R}}{2}\left(\frac{f}{\mathcal{R}} - f_{\mathcal{R}}\right) - \mathcal{L}_m f_{\mathcal{T}} \right. \\ &\left. - \frac{1}{2}\nabla_\lambda\nabla_\eta(f_{\mathcal{Q}}\mathcal{T}^{\lambda\eta})\right\} g_{\chi\xi} \\ &- \frac{1}{2}\Box(f_{\mathcal{Q}}\mathcal{T}_{\chi\xi}) - (g_{\chi\xi}\Box - \nabla_\chi\nabla_\xi) f_{\mathcal{R}} \\ &- 2f_{\mathcal{Q}}\mathcal{R}_{\lambda(\chi}\mathcal{T}^{\lambda}_{\xi)} + \nabla_\lambda\nabla_{(\chi}[\mathcal{T}^{\lambda}_{\xi)}f_{\mathcal{Q}}] \\ &+ 2(f_{\mathcal{Q}}\mathcal{R}^{\lambda\eta} + f_{\mathcal{T}}g^{\lambda\eta})\frac{\partial^2\mathcal{L}_m}{\partial g^{\chi\xi}\partial g^{\lambda\eta}}\Bigg], \end{aligned} \quad (3)$$

where

$$f_{\mathcal{R}} = \frac{\partial f(\mathcal{R}, \mathcal{T}, \mathcal{Q})}{\partial \mathcal{R}}, \quad f_{\mathcal{T}} = \frac{\partial f(\mathcal{R}, \mathcal{T}, \mathcal{Q})}{\partial \mathcal{T}}$$

and

$$f_{\mathcal{Q}} = \frac{\partial f(\mathcal{R}, \mathcal{T}, \mathcal{Q})}{\partial \mathcal{Q}}.$$

Moreover, the symbol ∇_χ defines the covariant derivative and $\Box \equiv g^{\chi\xi}\nabla_\chi\nabla_\xi$. We assume $\mathcal{L}_m = -\mu$ in this case, where μ indicates the energy density of the fluid which leads to $\frac{\partial^2\mathcal{L}_m}{\partial g^{\chi\xi}\partial g^{\lambda\eta}} = 0$ [20]. Due to the presence of arbitrary coupling between matter and geometry, the divergence of EMT (i.e., $\nabla_\chi\mathcal{T}^{\chi\xi} \neq 0$) in this theory does not disappear unlike GR and $f(\mathcal{R})$ theory. Thus, the equivalence principle is violated due to which there exists an additional force in the structure which prevents the moving particles to obey geodesic path in the gravitational field. Hence we get

$$\begin{aligned}\nabla^\chi\mathcal{T}_{\chi\xi} = &\frac{2}{2f_{\mathcal{T}} + \mathcal{R}f_{\mathcal{Q}} + 16\pi} \\ &\times\Bigg[\nabla_\chi(f_{\mathcal{Q}}\mathcal{R}^{\lambda\chi}\mathcal{T}_{\lambda\xi}) - \frac{1}{2}(f_{\mathcal{T}}g_{\lambda\eta} + f_{\mathcal{Q}}\mathcal{R}_{\lambda\eta})\nabla_\xi\mathcal{T}^{\lambda\eta} \\ &+ \nabla_\xi(\mathcal{L}_m f_{\mathcal{T}}) - \mathcal{G}_{\chi\xi}\nabla^\chi(f_{\mathcal{Q}}\mathcal{L}_m) \\ &- \frac{1}{2}\left\{\nabla^\chi(\mathcal{R}f_{\mathcal{Q}}) + 2\nabla^\chi f_{\mathcal{T}}\right\}\mathcal{T}_{\chi\xi}\Bigg]. \end{aligned} \quad (4)$$

The EMT characterises the matter configuration in the astrophysical structures and each of its non-null components expresses different physical characteristics. The anisotropy induced by the difference between pressure components in radial and tangential directions is observed as an important ingredient to study the formation and evolution of self-gravitating strange bodies. There are many massive objects in the Universe which are found to be coupled with anisotropic configuration. Thus, this factor has convincing consequences in the evolutionary stages of stellar structures. We consider anisotropic configured stars for which the EMT is defined as

$$\mathcal{T}^{(m)}_{\chi\xi} = (\mu + P_\perp)\mathcal{K}_\chi\mathcal{K}_\xi + P_\perp g_{\chi\xi} + (P_r - P_\perp)\mathcal{W}_\chi\mathcal{W}_\xi, \quad (5)$$

where P_r and $P_\perp$ indicate the radial and tangential pressures, respectively. Also, $\mathcal{K}_\chi$ is the four-velocity and $\mathcal{W}_\chi$ denotes the four-vector. The field equations in $f(\mathcal{R}, \mathcal{T}, \mathcal{Q})$ theory provide the trace as

$$\begin{aligned}&3\nabla^\lambda\nabla_\lambda f_{\mathcal{R}} + \mathcal{R}\left(f_{\mathcal{R}} - \frac{\mathcal{T}}{2}f_{\mathcal{Q}}\right) - \mathcal{T}(f_{\mathcal{T}} + 8\pi) \\ &+ \frac{1}{2}\nabla^\lambda\nabla_\lambda(f_{\mathcal{Q}}\mathcal{T}) + \nabla_\chi\nabla_\lambda(f_{\mathcal{Q}}\mathcal{T}^{\chi\lambda}) \\ &- 2f + (\mathcal{R}f_{\mathcal{Q}} + 4f_{\mathcal{T}})\mathcal{L}_m + 2\mathcal{R}_{\chi\lambda}\mathcal{T}^{\chi\lambda}f_{\mathcal{Q}} \\ &- 2g^{\xi\eta}\frac{\partial^2\mathcal{L}_m}{\partial g^{\xi\eta}\partial g^{\chi\lambda}}\left(f_{\mathcal{T}}g^{\chi\lambda} + f_{\mathcal{Q}}R^{\chi\lambda}\right) = 0. \end{aligned}$$

In a stellar object, the strong matter–geometry coupling disappears by assuming $\mathcal{Q} = 0$ in the above equation. Thus, we get $f(\mathcal{R}, \mathcal{T})$ theory, whereas the consideration of vacuum scenario provides the $f(\mathcal{R})$ theory.

The spherically symmetric geometry under consideration contains inner and outer regions separated by the hypersurface Σ. We take a metric which expresses static matter configuration corresponding to the inner space–time as follows:

$$ds^2 = -e^{\phi}dt^2 + e^{\psi}dr^2 + r^2d\theta^2 + r^2\sin^2\theta d\phi^2, \quad (6)$$

where $\phi = \phi(r)$ and $\psi = \psi(r)$. We assume co-moving framework for our analysis. Thus, the four-velocity and four-vector have the only non-zero components as

$$\mathcal{K}^{\chi} = \delta_0^{\chi}e^{-\phi/2}, \quad \mathcal{W}^{\chi} = \delta_1^{\chi}e^{-\psi/2}, \quad (7)$$

which must satisfy $\mathcal{K}^{\chi}\mathcal{K}_{\chi} = -1$ and $\mathcal{W}^{\chi}\mathcal{K}_{\chi} = 0$. There exist numerous stars in non-linear regime in the current evolutionary phase of our Universe. We need to study the linear behaviour of such objects to obtain a comprehensive description of their structural formation. As this theory encompasses the more complex functional, we adopt a separable model suggested by Haghani *et al* [17] to analyse the influence of $\mathcal{Q} = \mathcal{R}_{\chi\xi}\mathcal{T}^{\chi\xi}$ on different quark candidates as

$$f(\mathcal{R}, \mathcal{T}, \mathcal{Q}) = f_1(\mathcal{R}) + f_2(\mathcal{Q}). \quad (8)$$

We consider $f_1(\mathcal{R}) = \mathcal{R}$ and $f_2(\mathcal{Q}) = \varrho\mathcal{Q}$, where ϱ is an arbitrary coupling constant.

It is noticeable that different choices of the coupling parameters for physically feasible models should lie in their observed limits. This model has widely been used to study the stability and viability of various anisotropic solutions [18,19,23]. Here,

$$\mathcal{Q} = e^{-\psi}\left[\frac{\mu}{4}\left(\phi'^2 - \phi'\psi' + 2\phi'' + \frac{4\phi'}{r}\right) - \frac{P_r}{4}\left(\phi'^2 - \phi'\psi' + 2\phi'' + \frac{4\psi'}{r}\right) + P_{\perp}\left(\frac{\psi'}{r} - \frac{\phi'}{r} + \frac{2e^{\psi}}{r^2} - \frac{2}{r^2}\right)\right].$$

By inserting a particular model (8) in eq. (2) and combining it with eq. (3), we obtain

$$\mathcal{G}_{\chi\xi} = \frac{1}{\varrho\mu + 1}\left[\left(8\pi + \frac{1}{2}\varrho\mathcal{R}\right)\mathcal{T}^{(m)}_{\chi\xi} + \frac{\varrho}{2}\left\{\mathcal{Q} - \nabla_{\lambda}\nabla_{\eta}\mathcal{T}^{\lambda\eta}\right\}g_{\chi\xi} - \frac{\varrho}{2}\Box\mathcal{T}_{\chi\xi} - 2\varrho\mathcal{R}_{\lambda(\chi}\mathcal{T}^{\lambda}_{\xi)} + \varrho\nabla_{\lambda}\nabla_{(\chi}\mathcal{T}^{\lambda}_{\xi)}\right]. \quad (9)$$

The covariant divergence (4) for the considered model takes the form

$$\nabla^{\chi}\mathcal{T}_{\chi\xi} = \frac{2\varrho}{\varrho\mathcal{R} + 16\pi} \times \left[\nabla_{\chi}(\mathcal{R}^{\lambda\chi}\mathcal{T}_{\lambda\xi}) - \frac{1}{2}\mathcal{R}_{\lambda\eta}\nabla_{\xi}\mathcal{T}^{\lambda\eta} - \frac{1}{2}\mathcal{T}_{\chi\xi}\nabla^{\chi}\mathcal{R} - \mathcal{G}_{\chi\xi}\nabla^{\chi}\mathcal{L}_m\right]. \quad (10)$$

By using eqs (5) and (9) along with geometry (6), the field equations in this theory become

$$8\pi\mu = e^{-\psi}\left[\frac{\psi'}{r} + \frac{e^{\psi}}{r^2} - \frac{1}{r^2} + \varrho\left\{\mu\left(\frac{3\phi'\psi'}{8} - \frac{\phi'^2}{8} + \frac{2\psi'}{r} + \frac{2e^{\psi}}{r^2} - \frac{2}{r^2} - \frac{3\phi''}{4} - \frac{3\phi'}{2r}\right) - \mu'\left(\frac{\psi'}{4} - \frac{1}{r} - \phi'\right) + \frac{\mu''}{2} - P_r\left(\frac{\phi'^2}{8} - \frac{\phi'\psi'}{8} + \frac{\phi''}{4} - \frac{\psi'}{2r} - \frac{\psi''}{2} + \frac{3\psi'^2}{4}\right) + \frac{5\psi'P_r'}{4} - \frac{P_r''}{2} + P_{\perp}\left(\frac{\psi'}{2r} - \frac{\phi'}{2r} + \frac{e^{\psi}}{r^2} + \frac{1}{r^2}\right) - \frac{P_{\perp}'}{r}\right\}\right], \quad (11)$$

$$8\pi P_r = e^{-\psi}\left[\frac{\phi'}{r} - \frac{e^{\psi}}{r^2} + \frac{1}{r^2} + \varrho\left\{\mu\left(\frac{\phi'\psi'}{8} + \frac{\phi'^2}{8} - \frac{\phi''}{4} + \frac{\phi'}{2r} - \frac{e^{\psi}}{r^2} + \frac{1}{r^2}\right) - \frac{\phi'\mu'}{4} - P_r\left(\frac{5\phi'^2}{8} - \frac{7\phi'\psi'}{8} + \frac{5\phi''}{4} - \frac{7\psi'}{2r} + \frac{\phi'}{r} - \psi'^2 - \frac{e^{\psi}}{r^2} + \frac{1}{r^2}\right) + P_r' \times \left(\frac{\phi'}{4} + \frac{1}{r}\right) - P_{\perp}\left(\frac{\psi'}{2r} - \frac{\phi'}{2r} + \frac{e^{\psi}}{r^2} + \frac{1}{r^2}\right) + \frac{P_{\perp}'}{r}\right\}\right], \quad (12)$$

$$8\pi P_{\perp} = e^{-\psi}\left[\frac{\phi'^2}{4} - \frac{\phi'\psi'}{4} + \frac{\phi''}{2} - \frac{\psi'}{2r} + \frac{\phi'}{2r} + \varrho\left\{\mu\left(\frac{3\phi'^2}{8} - \frac{\phi'\psi'}{8} + \frac{\phi''}{4} - \frac{\psi'}{2r}\right) - \frac{\phi'\mu'}{4} + P_r\left(\frac{\phi'^2}{8} - \frac{\phi'\psi'}{8} + \frac{\phi''}{4} - \frac{\psi'}{2r} - \frac{\psi''}{2} + \frac{3\psi'^2}{4}\right) - \frac{5\psi'P_r'}{4} + \frac{P_r''}{2}\right.$$

$$- P_{\perp}\left(\frac{\phi'^2}{4} - \frac{\phi'\psi'}{4} + \frac{\phi''}{2} - \frac{\psi'}{r} + \frac{\phi'}{r} - \frac{2\mathrm{e}^{\psi}}{r^2} + \frac{1}{r^2}\right) - P'_{\perp}\left(\frac{\psi'}{4} - \frac{\phi'}{4} - \frac{3}{r}\right) + \frac{P''_{\perp}}{2}\Bigg\}\Bigg], \tag{13}$$

where the matter variables on the right side of eqs (11)–(13) appear due to the modified gravity which make the system more complicated. Here, prime symbolises $\partial/\partial r$. The expression for hydrostatic equilibrium in $f(\mathcal{R}, \mathcal{T}, \mathcal{Q})$ scenario is obtained with the help of eq. (10) as

$$\begin{aligned}
&\frac{\mathrm{d}P_r}{\mathrm{d}r} + \frac{\phi'}{2}(\mu + P_r) - \frac{2}{r}(P_{\perp} - P_r) \\
&- \frac{2\varrho\mathrm{e}^{-\psi}}{\varrho\mathcal{R} + 16\pi}\Bigg[\frac{\phi'\mu}{8}\left(\phi'^2 - \phi'\psi' + 2\phi'' + \frac{4\phi'}{r}\right) \\
&- \frac{\mu'}{8}\left(\phi'^2 - \phi'\psi' + 2\phi'' - \frac{4\phi'}{r} - \frac{8\mathrm{e}^{\psi}}{r^2} + \frac{8}{r^2}\right) \\
&+ P_r\left(\frac{5\phi'^2\psi'}{8} - \frac{5\phi'\psi'^2}{8} - \frac{5\psi'^2}{2r}\right. \\
&+ \frac{7\phi''\psi'}{4} + \frac{\phi'\psi''}{2} - \phi'\phi'' - \frac{\phi'''}{2} \\
&\left.+ \frac{2\psi''}{r} + \frac{\phi'\psi'}{r} - \frac{\psi'}{r^2} - \frac{\phi''}{r} + \frac{\phi'}{r^2} + \frac{2\mathrm{e}^{\psi}}{r^3} - \frac{2}{r^3}\right) \\
&+ \frac{P'_r}{8}\left(\phi'\psi' - \phi'^2 - 2\phi'' + \frac{4\psi'}{r}\right) \\
&+ \frac{P_{\perp}}{r^2}\left(\psi' - \phi' + \frac{2\mathrm{e}^{\psi}}{r} - \frac{2}{r}\right) \\
&- \frac{P'_{\perp}}{r}\left(\frac{\psi'}{2} - \frac{\phi'}{2} + \frac{\mathrm{e}^{\psi}}{r} - \frac{1}{r}\right)\Bigg] = 0.
\end{aligned} \tag{14}$$

The generalisation of Tolman–Opphenheimer–Volkoff (TOV) equation in this theory is illustrated by eq. (14). This equation seems to be very significant for studying the structural evolution of self-gravitating bodies.

The matter variables of the fluid distribution can be interlinked through different constraints, known as EoS which help to study the physical aspects of a stellar body. The most fascinating objects in our Universe are the neutron stars which are formed after the collapse of heavy structures having masses 8 to 20 times more than the mass of the Sun. The sufficiently dense stars can further be turned into black holes, while the less dense transform into quark stars whose conversion has been examined by various researchers [43,57]. These stars are found to be small in size, highly dense and occupy strong gravitational field. Due to non-linearity in field equations (11)–(13) involving five unknowns (ϕ, ψ, μ, P_r, $P_{\perp}$), we need some constraints to make the system solvable. We suppose that the matter variables in the interior of compact models are interlinked through MIT bag model EoS which plays a considerable role to analyse quark stars [33]. We define quark pressure as

$$P_r = \sum_{k=u,d,s} P^k - \mathfrak{B}_{\mathfrak{c}}, \tag{15}$$

where $\mathfrak{B}_{\mathfrak{c}}$ is the bag constant. Also, the pressures P^u, P^d and P^s correspond to the up, down and strange quark matters, respectively. Each quark density is interlinked with respective quark pressure as $\mu^k = 3P^k$. Thus, the energy density is expressed as

$$\mu = \sum_{k=u,d,s} \mu^k + \mathfrak{B}_{\mathfrak{c}}. \tag{16}$$

We construct MIT bag model EoS which illustrates strange matter by combining eqs (15) and (16) as

$$P_r = \frac{1}{3}(\mu - 4\mathfrak{B}_{\mathfrak{c}}). \tag{17}$$

Various researchers [58,59] analysed the physical characteristics of quark stars successfully by taking different values of the bag constant for the above EoS. Our main purpose is to find analytic solution of the field equations. Thus, after using the EoS (17) in eqs (11)–(13), we have

$$\begin{aligned}
\mu = &\Bigg[8\pi\mathrm{e}^{\psi} + \varrho\left(\frac{9\phi''}{8} - \frac{\mathrm{e}^{\psi}}{r^2} + \frac{1}{r^2} - \frac{\psi''}{8} - \frac{5\phi'\psi'}{8}\right. \\
&\left.- \frac{\psi'^2}{16} - \frac{5\psi'}{2r} + \frac{3\phi'^2}{16} + \frac{\phi'}{r}\right)\Bigg]^{-1} \\
&\times\Bigg[\frac{3}{4}\left(\frac{\psi'}{r} + \frac{\phi'}{r}\right) + \mathfrak{B}_{\mathfrak{c}}\Bigg\{8\pi\mathrm{e}^{\psi} \\
&- \varrho\left(\frac{\psi''}{2} + \frac{4\psi'}{r} - \frac{3\phi'^2}{4} - \frac{3\phi''}{2}\right. \\
&\left.+ \frac{\psi'^2}{4} - \frac{\phi'}{r} + \frac{\mathrm{e}^{\psi}}{r^2} + \phi'\psi' - \frac{1}{r^2}\right)\Bigg\}\Bigg],
\end{aligned} \tag{18}$$

$$\begin{aligned}
P_r = &\Bigg[8\pi\mathrm{e}^{\psi} + \varrho\left(\frac{9\phi''}{8} - \frac{\mathrm{e}^{\psi}}{r^2} + \frac{1}{r^2} - \frac{\psi''}{8}\right. \\
&\left.- \frac{5\phi'\psi'}{8} - \frac{\psi'^2}{16} - \frac{5\psi'}{2r} + \frac{3\phi'^2}{16} + \frac{\phi'}{r}\right)\Bigg]^{-1} \\
&\times\Bigg[\frac{1}{4}\left(\frac{\psi'}{r} + \frac{\phi'}{r}\right) - \mathfrak{B}_{\mathfrak{c}}\Bigg\{8\pi\mathrm{e}^{\psi} \\
&- \varrho\left(\frac{\phi'\psi'}{2} + \frac{2\psi'}{r} - \frac{\phi'}{r} + \frac{\mathrm{e}^{\psi}}{r^2}\right. \\
&\left.- \phi'' - \frac{1}{r^2}\right)\Bigg\}\Bigg],
\end{aligned} \tag{19}$$

$$P_{\perp} = \left[8\pi\mathrm{e}^{\psi} + \varrho\left(\frac{\phi'^2}{4} - \frac{2\mathrm{e}^{\psi}}{r^2} + \frac{1}{r^2} - \frac{\phi'\psi'}{4} + \frac{\phi''}{2}\right.\right.$$

$$
\begin{aligned}
&-\frac{\psi'}{r}+\frac{\phi'}{r}\Big)\Big]^{-1}\Big[\frac{\phi'^2}{4}-\frac{\psi'}{2r}+\frac{\phi'}{2r}-\frac{\phi'\psi'}{4}+\frac{\phi''}{2}\\
&+\varrho\Big\{8\pi e^{\psi}+\varrho\Big(\frac{9\phi''}{8}-\frac{e^{\psi}}{r^2}+\frac{1}{r^2}-\frac{\psi''}{8}\\
&-\frac{5\phi'\psi'}{8}-\frac{\psi'^2}{16}-\frac{5\psi'}{2r}+\frac{3\phi'^2}{16}+\frac{\phi'}{r}\Big)\Big\}^{-1}\\
&\times\Big\{\frac{1}{16r}\Big(\phi'\psi'^2+3\phi'^2\psi'+5\phi'^3+4\phi''\psi'\\
&+4\phi'\phi''-2\psi'\psi''-2\phi'\psi''+3\psi'^3-\frac{8\psi'^2}{r}-\frac{8\phi'\psi'}{r}\Big)\\
&+2\pi e^{\psi}\mathfrak{B}_c(\phi'^2+2\psi''-3\psi'^2)\\
&+\frac{\varrho\mathfrak{B}_c}{16}\Big(4\phi''\psi''-11\phi''\psi'^2-3\phi'^2\psi''\\
&+10\phi''\phi'^2-3\phi'\psi'\psi''-3\phi'\phi''\psi'\\
&+2\phi'^2+\frac{5\phi'^2\psi'^2}{2}-\frac{13\phi'^3\psi'}{2}-\frac{4\phi'\psi'^2}{r}\\
&+\frac{11\phi'\psi'^3}{2}-\frac{26\phi'^2\psi'}{r}-\frac{12\phi''\psi'}{r}\\
&+\frac{4\phi'^3}{r}-\frac{12\psi'\psi''}{r}+\frac{22\psi'^3}{r}+\frac{9\phi'^4}{2}\\
&-\frac{4\phi'^2e^{\psi}}{r^2}+\frac{4\phi'^2}{r^2}-\frac{8\psi''e^{\psi}}{r^2}-\frac{12\psi'^2e^{\psi}}{r^2}\\
&+\frac{8\psi''}{r^2}+\frac{4\psi'^2}{r^2}\Big)\Big\}\Big]. \qquad (20)
\end{aligned}
$$

2.1 *Krori–Barua solution*

Various researchers utilised EoS (17) to explore the physical features of different quark stars in both GR as well as modified framework. Our aim is to develop anisotropic solution by means of such a simple EoS and analyse its feasibility corresponding to five star candidates. To do this, we consider Krori–Barua solution [60] in $f(\mathcal{R},\mathcal{T},\mathcal{Q})$ scenario which has acquired a lot of attention due to its singularity-free nature. The solution has the form

$$\phi=Br^2+C,\quad \psi=Ar^2, \qquad (21)$$

where A, B and C are unknowns and their values can be calculated through matching conditions. Now, we check the criteria for acceptability of these metric coefficients [61], thus their first and second derivatives are

$$
\begin{aligned}
&\phi'(r)=2Br,\quad \psi'(r)=2Ar,\\
&\phi''(r)=2B,\quad \psi''(r)=2A,
\end{aligned}
$$

from where we observe that $\phi'(0)=\psi'(0)=0$, $\phi''(0)>0$ and $\psi''(0)>0$ everywhere ($r=0$ is the centre of the star). Hence, both the metric potentials given in eq. (21) are acceptable. Field equations (18)–(20) in the Krori–Barua framework (21) become

$$
\begin{aligned}
\mu=&[\varrho(-A^2r^4-Ar^2\left(10Br^2+21\right)\\
&+3B^2r^4+17Br^2+4)+32\pi r^2e^{Ar^2}-4\varrho e^{Ar^2}]^{-1}\\
&\times[2\left(-2\varrho A^2\mathfrak{B}_c r^4+Ar^2\left(3-2\varrho\mathfrak{B}_c\left(4Br^2+9\right)\right)\right.\\
&+2\mathfrak{B}_c\left(\varrho+e^{Ar^2}\left(8\pi r^2-\varrho\right)\right)\\
&\left.+6\varrho\mathfrak{B}_cB^2r^4+Br^2(10\varrho\mathfrak{B}_c+3)\right)], \qquad (22)\\
P_r=&[\varrho(-A^2r^4-Ar^2\left(10Br^2+21\right)\\
&+3B^2r^4+17Br^2+4)+32\pi r^2e^{Ar^2}-4\varrho e^{Ar^2}]^{-1}\\
&\times[2\left(Ar^2\left(4\varrho\mathfrak{B}_c\left(Br^2+2\right)+1\right)\right.\\
&\left.-2\mathfrak{B}_c(\varrho+e^{Ar^2}(8\pi r^2-\varrho))+Br^2(1-8\varrho\mathfrak{B}_c)\right)], \qquad (23)\\
P_\perp=&[\{\varrho\left(-Ar^2\left(Br^2+2\right)+B^2r^4+3Br^2+1\right)\\
&+e^{Ar^2}\left(8\pi r^2-\varrho\right)\}\{\varrho(4A^2r^4-Ar^2\left(10Br^2+21\right)\\
&+3B^2r^4+17Br^2)+4e^{Ar^2}\left(8\pi r^2-\varrho\right)\}]^{-1}\\
&\times[r^2\{\varrho A^3r^4\left(44\varrho\mathfrak{B}_c+Br^2(22\varrho\mathfrak{B}_c+1)+7\right)\\
&-\varrho A^2r^2\left(8\varrho\mathfrak{B}_c+4\mathfrak{B}_ce^{Ar^2}\left(\varrho+24\pi r^2\right)\right.\\
&\left.-B^2r^4(10\varrho\mathfrak{B}_c+9)-Br^2(31-36\varrho\mathfrak{B}_c)-11\right)\\
&+B\left(4e^{Ar^2}\left(8\pi r^2-\varrho\right)\left(Br^2(\varrho\mathfrak{B}_c+1)+2\right)\right.\\
&+\varrho\left(3B^3r^6(6\varrho\mathfrak{B}_c+1)+B^2r^4(28\varrho\mathfrak{B}_c+33)\right.\\
&\left.\left.+6Br^2(\varrho\mathfrak{B}_c+7)+8\right)\right)\\
&-A\left(4e^{Ar^2}\left(8\pi r^2-\varrho\right)\left(-\varrho\mathfrak{B}_c+Br^2+1\right)\right.\\
&+\varrho\left(13B^3r^6(2\varrho\mathfrak{B}_c+1)+B^2r^4(64\varrho\mathfrak{B}_c+55)\right.\\
&\left.\left.+Br^2(8\varrho\mathfrak{B}_c+69)-4\varrho\mathfrak{B}_c+4\right)\right)\}]. \qquad (24)
\end{aligned}
$$

3. Boundary conditions

To analyse the exact structural configuration of anisotropic compact stars, the existence of smooth matching between inner and outer geometries plays significant

role. We take the outer Schwarzschild space–time in this context which is symbolised by the metric as

$$\mathrm{d}s^2 = -\left(1-\frac{2\bar{M}}{r}\right)\mathrm{d}t^2 + \left(1-\frac{2\bar{M}}{r}\right)^{-1}\mathrm{d}r^2 + r^2\mathrm{d}\theta^2 + r^2\sin^2\theta\,\mathrm{d}\varphi^2, \tag{25}$$

where $\bar{M}$ indicates the mass of the exterior geometry. The continuity of the metric coefficients of both geometries at the boundary surface produces some constraints as

$$g_{tt} = \mathrm{e}^{B\mathcal{H}^2+C} = 1-\frac{2\bar{M}}{\mathcal{H}}, \tag{26}$$

$$g_{rr} = \mathrm{e}^{-A\mathcal{H}^2} = 1-\frac{2\bar{M}}{\mathcal{H}}, \tag{27}$$

$$\frac{\partial g_{tt}}{\partial r} = B\mathcal{H}\mathrm{e}^{B\mathcal{H}^2+C} = \frac{\bar{M}}{\mathcal{H}^2}.$$

After solving the above three equations simultaneously, we obtain the values of triplet (A, B, C) as

$$A = -\frac{1}{\mathcal{H}^2}\ln\left(1-\frac{2\bar{M}}{\mathcal{H}}\right), \tag{28}$$

$$B = \frac{\bar{M}}{\mathcal{H}^3}\left(1-\frac{2\bar{M}}{\mathcal{H}}\right)^{-1}, \tag{29}$$

$$C = \ln\left(1-\frac{2\bar{M}}{\mathcal{H}}\right) - \frac{\bar{M}}{\mathcal{H}-2\bar{M}}. \tag{30}$$

The radial pressure in stellar structures must vanish at the boundary ($r = \mathcal{H}$). Thus, eq. (23) along with eqs (28)–(30) lead to the following expression:

$$\begin{aligned} P_r|_{(r=\mathcal{H})} &= \Bigg[15\varrho\bar{M}^2 + \varrho\left(-64\bar{M}^2 + 74\bar{M}\mathcal{H} - 21\mathcal{H}^2\right) \\ &\quad\times\log\left(1-\frac{2\bar{M}}{\mathcal{H}}\right) + 64\pi\bar{M}\mathcal{H}^3 - 9\varrho\bar{M}\mathcal{H} \\ &\quad+\varrho(\mathcal{H}-2\bar{M})^2\log^2\left(1-\frac{2\bar{M}}{\mathcal{H}}\right) - 32\pi\mathcal{H}^4\Bigg]^{-1} \\ &\quad\times\Bigg[2(2\bar{M}-\mathcal{H})\Bigg\{-4\varrho\mathfrak{B}_c\bar{M} + \log\left(1-\frac{2\bar{M}}{\mathcal{H}}\right) \\ &\quad\times(2\bar{M}(6\varrho\mathfrak{B}_c+1) - \mathcal{H}(8\varrho\mathfrak{B}_c+1)) \\ &\quad+\bar{M} - 16\pi\mathfrak{B}_c\mathcal{H}^3\Bigg\}\Bigg] = 0. \end{aligned} \tag{31}$$

The bag constant can be evaluated from eq. (31) as

$$\mathfrak{B}_c = \frac{(2\bar{M}-\mathcal{H})\log\left(1-\frac{2\bar{M}}{\mathcal{H}}\right) + \bar{M}}{2\left\{2\varrho\bar{M} + 2\varrho(2\mathcal{H}-3\bar{M})\log\left(1-\frac{2\bar{M}}{\mathcal{H}}\right) + 8\pi\mathcal{H}^3\right\}}. \tag{32}$$

By utilising the experimental data of different quark stars [62,63], the values of A, B, C and $\mathfrak{B}_c$ can be determined. These strange bodies are found to be consistent with the limit proposed by Buchdhal [64], i.e.,

$$\frac{2\bar{M}}{\mathcal{H}} < \frac{8}{9}.$$

We choose $\varrho = 3$ to find the value of bag constant for the considered model. This value of coupling constant helps us in the successful analysis of stellar evolution. The values of bag constant as well as three unknowns involved in the Krori–Barua solution corresponding to the observed masses and radii of the considered strange stars are calculated in tables 1 and 2, respectively.

Remarkably, we determine the values of $\mathfrak{B}_c$ for the different quark stars which are 105.03, 55.28, 200.55, 229.46 and 111.73 MeV/fm^3, respectively. The observed values of bag constant for these stars to be stable are much lesser than the above calculated values. However, the experimental findings released by CERN-SPS and RHIC show that the density-dependent bag model may yield a vast range of values of bag constant.

4. Physical analysis of various compact stars

This section examines different physical features of the considered strange stars which are coupled with anisotropic configuration in $f(\mathcal{R},\mathcal{T},\mathcal{Q})$ scenario. We observe the graphical behaviour of matter variables by using masses and radii of each star candidate as shown in table 1. We analyse the viability of metric potentials, energy density, radial and tangential components of pressure, anisotropy, energy bounds, compactness as well as red-shift for the considered quark candidates and also investigate their stability, where the model parameter has been kept fixed. We are familiar with the fact that the compatibility of a solution guarantees the non-singular and monotonically increasing nature of metric components, having positive values throughout. Equation (21) shows that the metric coefficients depend only on Krori–Barua constants. By utilising these constants for particular stars shown in table 2, the graphical behaviour of both metric functions is analysed in figure 1

Table 1. Physical values of different compact star candidates.

Star models	4U 1820-30	Vela X-I	SAX J 1808.4-3658	RXJ 1856-37	Her X-I
Mass ($M_{\odot}$)	2.25	1.77	1.435	0.9041	0.88
R (km)	10	12.08	7.07	6	7.7
M/R	0.331	0.215	0.298	0.222	0.168
$\mathfrak{B}_c$	0.000139001	0.000073158	0.000265408	0.000303665	0.000147867

Table 2. Calculated values of Krori–Barua constants A, B and C for different compact star candidates.

Star models	4U 1820-30	Vela X-I	SAX J 1808.4-3658	RXJ 1856-37	Her X-I
A	0.0108323	0.0038614	0.0181686	0.0162557	0.0069063
B	0.0097711	0.0025930	0.0148019	0.0110467	0.0042674
C	−2.06034	−0.94188	−1.64803	−0.98289	−0.66249

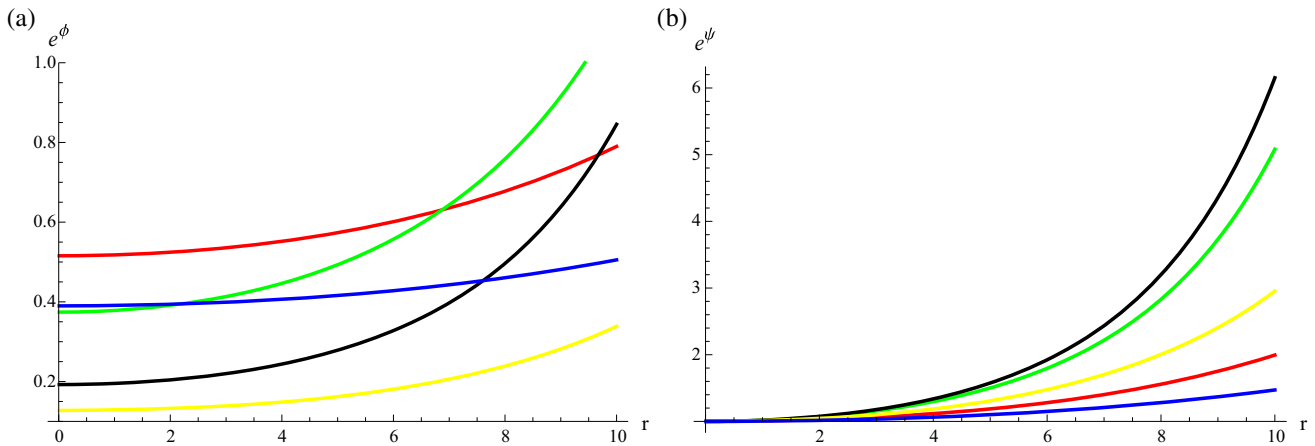

Figure 1. Behaviour of temporal (**a**) and radial (**b**) metric potentials vs. r for different compact star candidates.

which assures the physical consistency of the developed solution. It should be noted that the yellow colour expresses 4U 1820-30 compact star, blue indicates Vela X-I, black represents SAX J 1808.4-3658, green signifies RXJ 1856-37 and red shows Her X-I in all the plots.

4.1 *Inspection of physical parameters*

The composition of compact gravitational bodies indicates that the energy density and both pressure ingredients should be maximum at the centre of the stellar structure. Figure 2 shows the variation in these parameters with respect to each quark candidate for model (8). These graphs clearly demonstrate that the energy density and pressure components gain their maximum values at the centre ($r = 0$) of the anisotropic configured stars, resulting in the existence of extremely dense structures. Figure 2b also shows that the radial pressures inside the considered strange stars disappear at the boundary, while the energy density and tangential pressure decrease linearly with the rise in r. The matter variables fulfill

$$\frac{\mathrm{d}\mu}{\mathrm{d}r} < 0, \frac{\mathrm{d}P_r}{\mathrm{d}r} < 0$$

and

$$\frac{\mathrm{d}P_{\perp}}{\mathrm{d}r} < 0$$

as shown in figure 3, and thus they yield regular behaviour. We observe from this graphical analysis that there must exist highly compact stars having anisotropic configuration in $f(\mathcal{R}, \mathcal{T}, \mathcal{Q})$ gravity.

4.2 *Effect of anisotropic pressure*

We calculate the anisotropic factor in terms of Krori–Barua ansatz and bag constant $\mathfrak{B}_c$ using eqs (23) and (24) as

$$\begin{aligned}\Delta = [&\{\varrho\left(-Ar^2\left(Br^2+2\right)+B^2r^4+3Br^2+1\right)\\&+\mathrm{e}^{Ar^2}\left(8\pi r^2-\varrho\right)\}\\&\times\{\varrho\left(4A^2r^4-Ar^2\left(10Br^2+21\right)+3B^2r^4\right.\end{aligned}$$

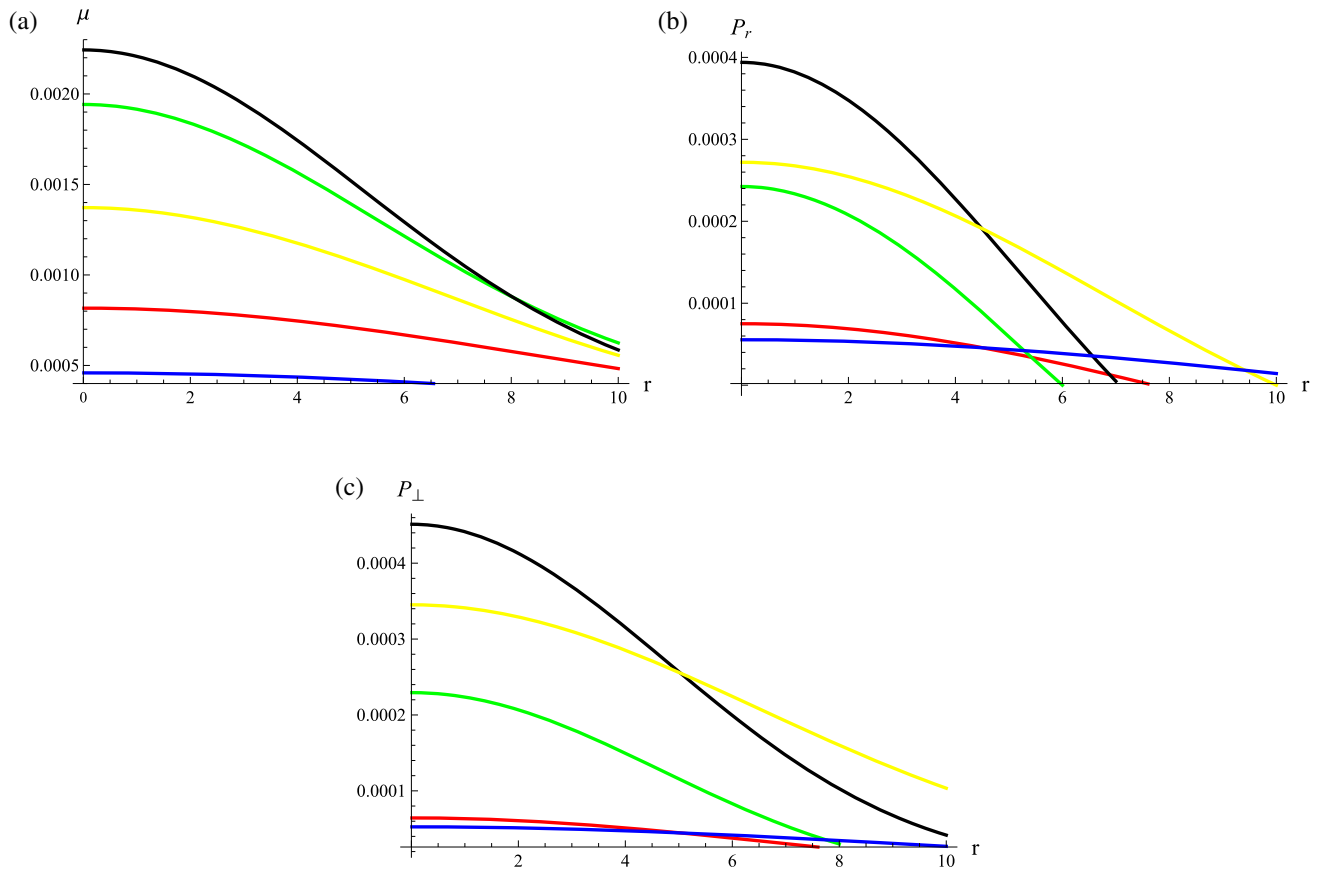

Figure 2. Plots of energy density (in km^{-2}) (**a**), radial pressure (in km^{-2}) (**b**) and tangential pressure (in km^{-2}) (**c**) vs. r for different compact star candidates.

$$
\begin{aligned}
&+17Br^2\big) + 4\mathrm{e}^{Ar^2}\left(8\pi r^2 - \varrho\right)\}]^{-1}\\
&\times [\varrho A^3 r^6\left(44\varrho\mathfrak{B}_\mathfrak{c} + Br^2(22\varrho\mathfrak{B}_\mathfrak{c} + 1) + 7\right)\\
&+ \varrho A^2 r^4\big(3(8\varrho\mathfrak{B}_\mathfrak{c} + 5) - 4\mathfrak{B}_\mathfrak{c}\mathrm{e}^{Ar^2}\\
&\times \left(\varrho + 24\pi r^2\right) + 9B^2 r^4(2\varrho\mathfrak{B}_\mathfrak{c} + 1)\\
&+ Br^2(33 - 4\varrho\mathfrak{B}_\mathfrak{c})\big) + 2B^2 r^4\big(\varrho(29\varrho\mathfrak{B}_\mathfrak{c} + 18)\\
&+ 2(2\varrho\mathfrak{B}_\mathfrak{c} + 1)\mathrm{e}^{Ar^2}\left(8\pi r^2 - \varrho\right)\big)\\
&- Ar^2\big(2\mathrm{e}^{Ar^2}\left(8\pi r^2 - \varrho\right)\\
&\times \left(3 + 2Br^2 \times (3\varrho\mathfrak{B}_\mathfrak{c} + 1) + 10\varrho\mathfrak{B}_\mathfrak{c}\right)\\
&+ \varrho\big(20\varrho\mathfrak{B}_\mathfrak{c} + B^3 r^6(34\varrho\mathfrak{B}_\mathfrak{c} + 13)\\
&+ 5B^2 r^4(24\varrho\mathfrak{B}_\mathfrak{c} + 11)\\
&+ Br^2(71 + 100\varrho\mathfrak{B}_\mathfrak{c}) + 6)\big)\\
&+ 4\mathfrak{B}_\mathfrak{c}\left(\varrho + \mathrm{e}^{Ar^2}\left(8\pi r^2 - \varrho\right)\right)^2 + 2Br^2\\
&\times \left(\varrho + \mathrm{e}^{Ar^2}\left(8\pi r^2 - \varrho\right)\right)(14\varrho\mathfrak{B}_\mathfrak{c} + 3)\\
&+ 3\varrho B^4 r^8(6\varrho\mathfrak{B}_\mathfrak{c} + 1) + \varrho B^3 r^6(44\varrho\mathfrak{B}_\mathfrak{c} + 31)].
\end{aligned}
\tag{33}
$$

We use the observational data of various considered stars (shown in table 1) to analyse the behaviour of anisotropy in their structural evolution. An outward directed anisotropic pressure occurs when $P_\perp > P_r$ which yields $\Delta > 0$. On the other hand, the condition $P_\perp < P_r$ (i.e., $\Delta < 0$) leads to the inward directed pressure. The effect of anisotropy on different stars is shown in figure 4 corresponding to the viable model of $f(\mathcal{R}, \mathcal{T}, \mathcal{Q})$ theory. It is noticed that Δ remains positive throughout only for 4U 1820-30 and SAX J 1808.4-3658 stars which assures that there exists a repelling force which contributes to the structural evolution of massive geometries, while this factor varies from negative to positive in the interior of the remaining three candidates.

4.3 *Mass, compactness and surface red-shift*

For spherical structures, the mass can be defined as

$$m(r) = \frac{1}{2}\int_0^{\mathcal{H}} r^2\mu\,\mathrm{d}r, \tag{34}$$

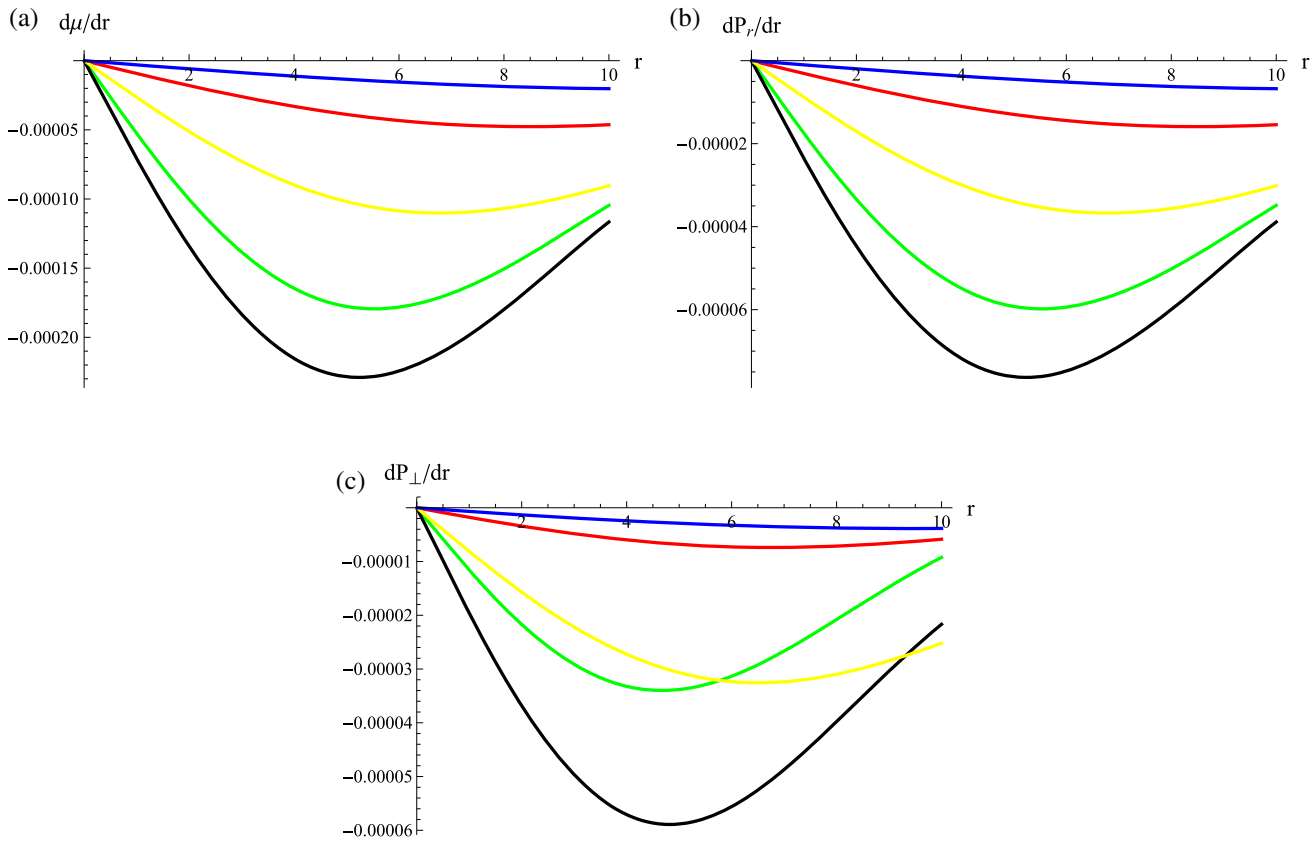

Figure 3. Plots of $\mathrm{d}\mu/\mathrm{d}r$ (in km^{-2}) (**a**), $\mathrm{d}P_r/\mathrm{d}r$ (in km^{-2}) (**b**) and $\mathrm{d}P_\perp/\mathrm{d}r$ (in km^{-2}) (**c**) vs. r for different compact star candidates.

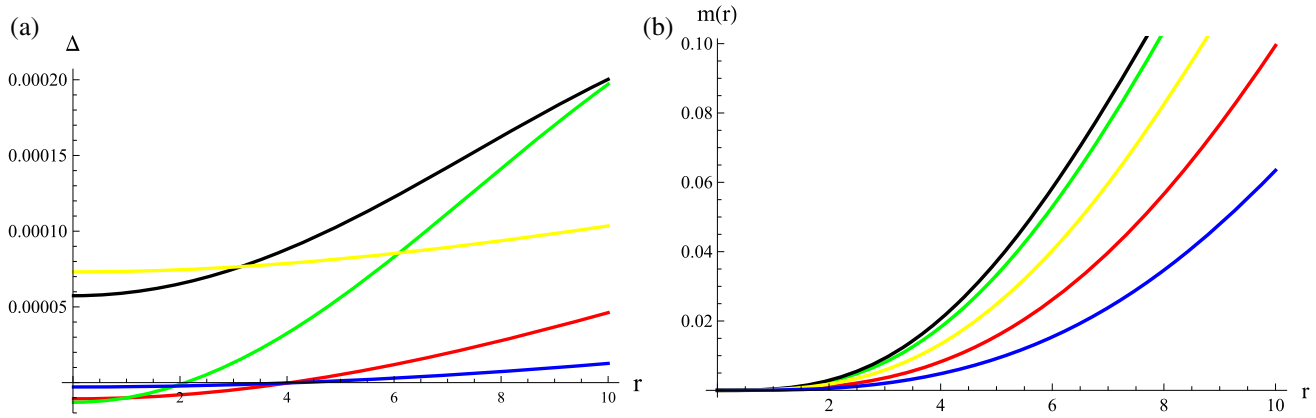

Figure 4. Variation of anisotropy (in km^{-2}) (**a**) and mass (in km) (**b**) vs. r for different compact star candidates.

where μ is given in eq. (22). For our proposed model, we analyse the graphical behaviour of the mass of the considered stars by solving eq. (34) numerically along with the initial condition $m(0) = 0$, as can be seen from figure 4. We can characterise a celestial structure by its different physical features, among them one is the compactness $\big(\sigma(r)\big)$ which is the ratio of mass and radius. After employing the matching conditions between the inner and outer space–times at $r = \mathcal{H}$, Buchdahl [64] found the upper bound of $\sigma(r)$. He disclosed that the system will remain stable until its value will not be greater than $4/9$. Some reactions occur in the core of a massive body (having a strong gravitational force) due to which the electromagnetic radiations diffuse from that body. The red-shift factor measures the increment in wavelength of those radiations. Mathematically, it is characterised as

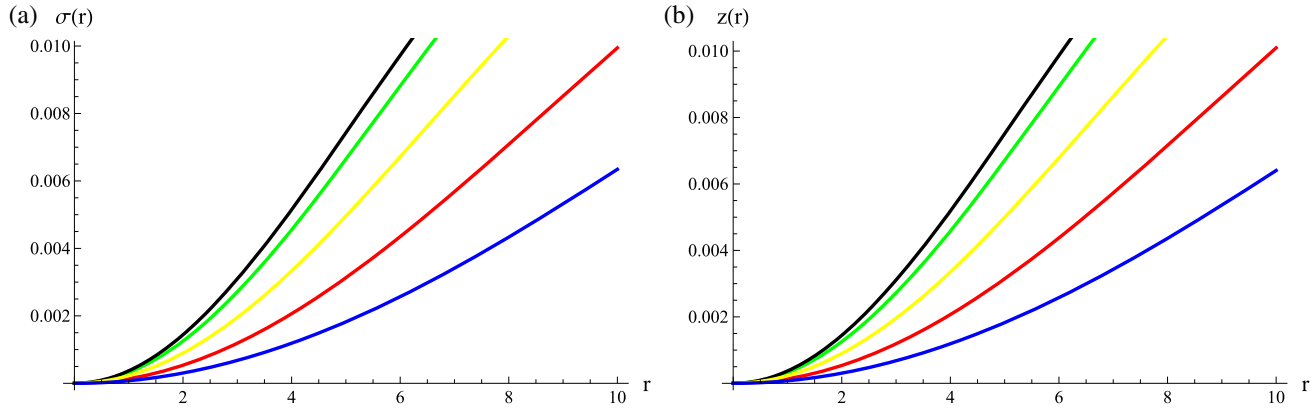

Figure 5. Variation of compactness (**a**) and red-shift (**b**) factors vs. r for different compact star candidates.

$$z(r) = \frac{1}{\sqrt{1-2\sigma}} - 1. \tag{35}$$

This factor plays an influential role for studying the particles existing in the inner geometry and its EoS. For perfect fluid distribution, Buchdahl found its value as $z(r) < 2$, whereas Ivanov [65] studied anisotropic compact stars and observed its upper limit to be 5.211. Figure 5 shows the plots for compactness as well as red-shift for all quark candidates. It can be seen that the values of both factors are in their desired ranges.

4.4 *Energy conditions*

The existence of matter configuration in a stellar body can be demonstrated by some bounds, known as energy conditions which are of great importance in astrophysics. We can distinguish the usual or exotic matter existing inside the geometry by employing such conditions. They also help to investigate the viability of the developed solutions in any gravitational theory. The physical parameters representing a particular geometry having ordinary matter must fulfill these conditions. The energy bounds for anisotropic configured star in $f(\mathcal{R}, \mathcal{T}, \mathcal{Q})$ gravity are

$$\begin{aligned} &\mu \geq 0, \quad \mu + P_r \geq 0, \\ &\mu + P_\perp \geq 0, \quad \mu - P_r \geq 0, \\ &\mu - P_\perp \geq 0, \quad \mu + P_r + 2P_\perp \geq 0. \end{aligned} \tag{36}$$

The plots of all the above conditions are shown in figure 6. It is found that these conditions possess positive trend, assuring the viability of the chosen model and the resulting solution. Thus, there must exist normal matter in the interior of all quark candidates.

4.5 *Stability analysis*

The stability of a compact star attains great significance in astrophysics to analyse physically feasible models. The massive bodies which show stable behaviour against all the external fluctuations are more intriguing, and thus this phenomenon has considerable interest in the study of their structural development. To analyse the stability of the considered candidates in $f(\mathcal{R}, \mathcal{T}, \mathcal{Q})$ gravity, we employ two approaches. One of them is the cracking concept presented by Herrera [36] which is based on the speed of sound. The causality condition declares that the squared sound speed

$$v_s^2 = \frac{\mathrm{d}P}{\mathrm{d}\mu}$$

should lie within $[0, 1]$, i.e., $0 \leq v_s^2 < 1$ throughout for stable structure. This becomes in the case of anisotropic matter as $0 \leq v_{sr}^2 < 1$ and $0 \leq v_{s\perp}^2 < 1$, where $v_{sr}^2 = (\mathrm{d}P_r/\mathrm{d}\mu)$ represents the radial and $v_{s\perp}^2 = (\mathrm{d}P_\perp/\mathrm{d}\mu)$ shows tangential ingredients of the speed of sound. Thus, the fulfilment of the inequality $0 \leq |v_{s\perp}^2 - v_{sr}^2| < 1$ guarantees the stability of compact object. Figure 7 shows that all the considered candidates are stable for their respective calculated values of bag constant and $\varrho = 3$.

Secondly, the adiabatic index (Γ) is considered as a powerful tool to analyse the stability of stellar geometry. This technique has been utilised to study the stable self-gravitating objects in which the adiabatic index should have its value greater than $4/3$ everywhere [66]. In this case, Γ is characterised as

$$\Gamma = \frac{\mu + P_r}{P_r}\left(\frac{\mathrm{d}P_r}{\mathrm{d}\mu}\right) = \frac{\mu + P_r}{P_r}\left(v_{sr}^2\right). \tag{37}$$

Figure 8 demonstrates the physical behaviour of Γ for all candidates which fully agrees with the desired limit throughout the structure.

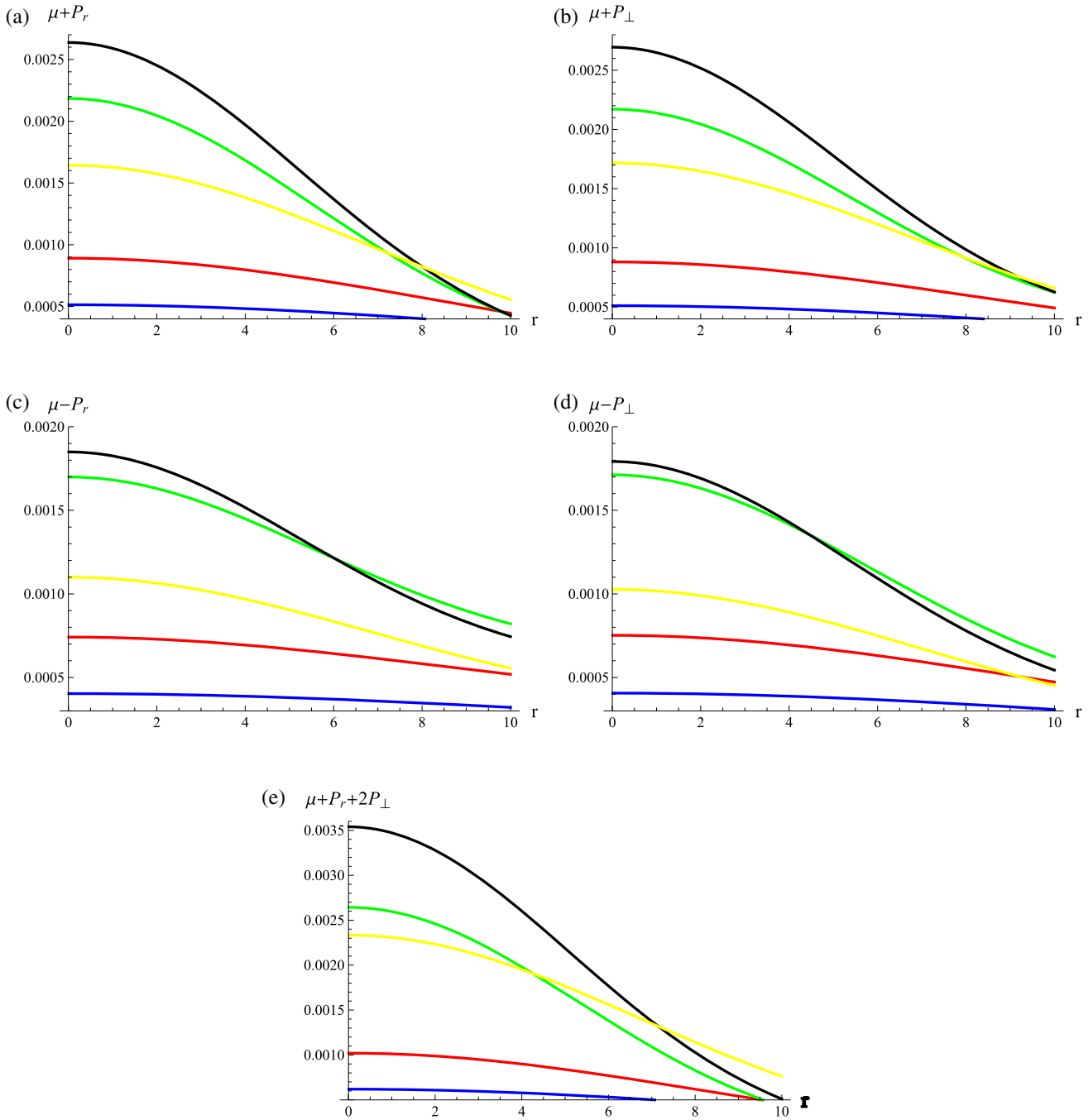

Figure 6. Plots of energy conditions (in km^{-2}) vs. r for different compact star candidates.

5. Conclusions

This paper discusses the effect of MIT bag constant ($\mathfrak{B}_c$) on the physical attributes of five different strange anisotropic stars, namely 4U 1820-30, Vela X-I, SAX J 1808.4-3658, RXJ 1856-37 and Her X-I in $f(\mathcal{R}, \mathcal{T}, \mathcal{Q})$ theory of gravity. We analyse the influence of strong non-minimal coupling between matter and geometry in this theory (which appears due to the factor $\mathcal{Q} = \mathcal{R}_{\chi\xi}\mathcal{T}^{\chi\xi}$) by adopting a linear model $\mathcal{R}+\varrho\mathcal{Q}$, where the coupling constant has been kept fixed as $\varrho = 3$. We have formulated the field equations as well as TOV equation using bag model EoS (17) and also calculated the values of $\mathfrak{B}_c$ corresponding to each star candidate (table 1). We have utilised the values of the metric potentials proposed by Krori–Barua involving three unknowns (A, B, C) whose values have been evaluated in terms of masses and radii through matching conditions in this theory. The

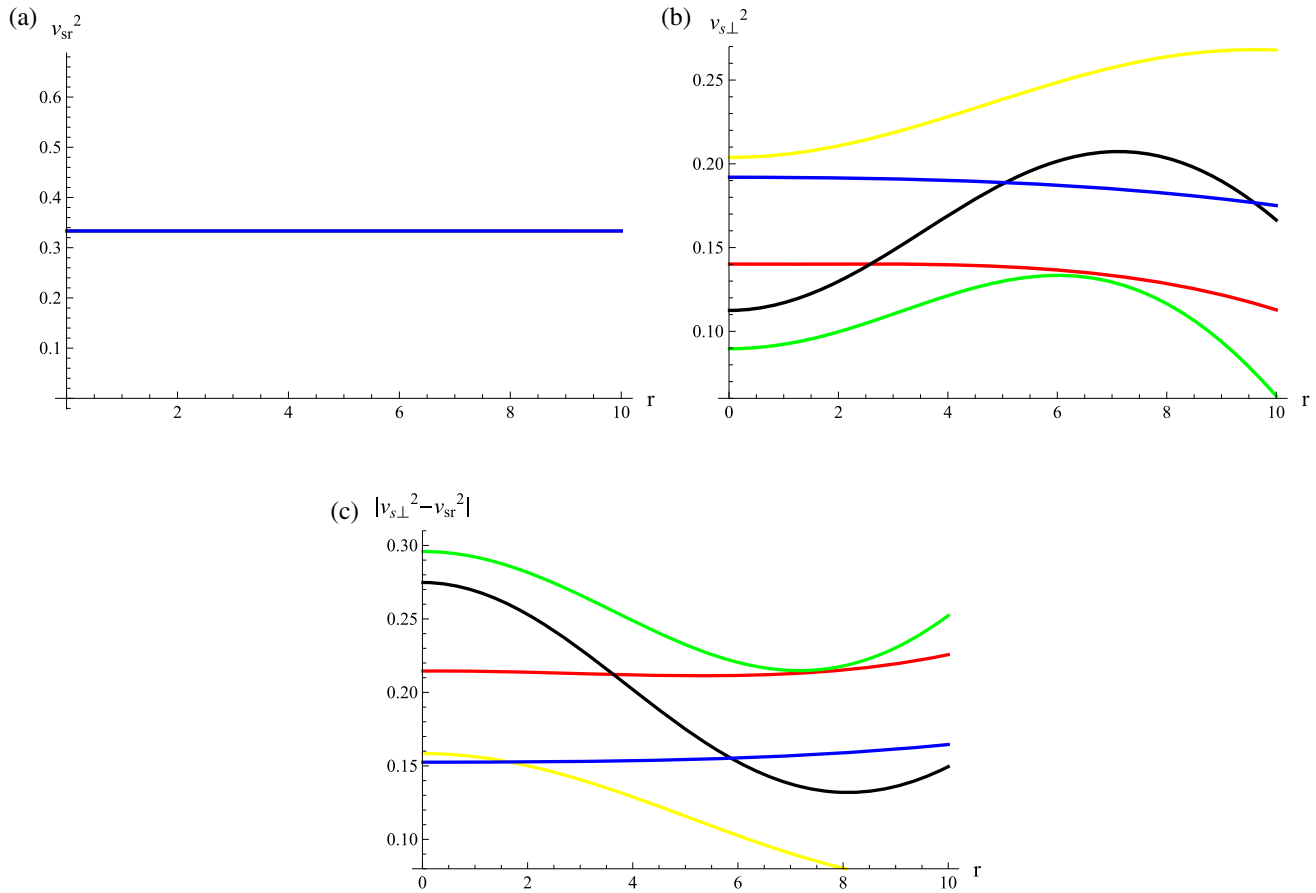

Figure 7. Plots of v_{sr}^2 (**a**), $v_{s\perp}^2$ (**b**) and $|v_{s\perp}^2 - v_{sr}^2|$ (**c**) vs. r for different compact star candidates.

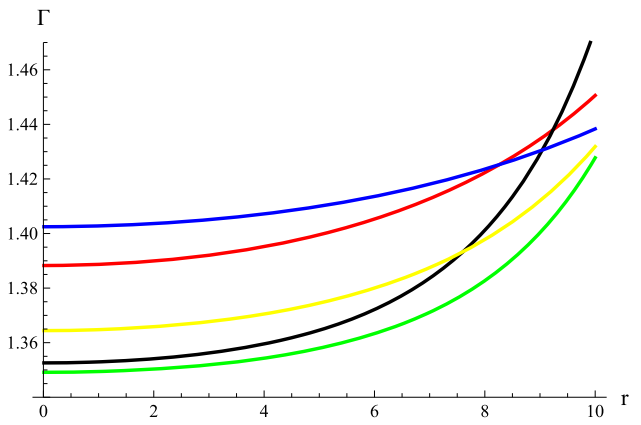

Figure 8. Plot of adiabatic index vs. r for different compact star candidates.

observational data of various star candidates have been used to calculate this triplet (table 2). We have found analytic solution of the modified field equations by taking two different EoSs relating energy density with pressure components. The graphical analyses of all quark candidates have been presented. It is found that the physical parameters attained their maximum (positive) values at the centre ($r = 0$), while the behaviour of anisotropy is increasing towards the boundary.

The observed values of red-shift and compactness are within their respective bounds. The energy conditions are fulfilled, confirming the existence of the usual matter inside the quark candidates as well as the viability of our developed solution. Two different techniques have been used to analyse the stability. We have determined that the potentially stable structure of these stars exist as the inequalities $0 \leq v_{sr}^2 < 1$, $0 \leq v_{s\perp}^2 < 1$ and $0 \leq |v_{s\perp}^2 - v_{sr}^2| < 1$ hold throughout the system. The adiabatic index for all the considered stars has been visualised which also assures their stable structures. It is worthwhile to note that the quark star 4U 1820-30 shows more stable behaviour towards the boundary than the other four candidates (figure 7). It is concluded that the non-minimal matter–geometry interaction in $f(\mathcal{R}, \mathcal{T}, \mathcal{Q})$ theory may yield more appropriate results for compact structures compared to [23,24]. We have found that the chosen model (8) has viable behaviour as the compact structures obtained with the help of MIT EoS (17) meet the needed requirements. Finally, we can

retrieve all these results in GR for $\varrho = 0$ in $f(\mathcal{R}, \mathcal{T}, \mathcal{Q})$ functional form (8).

Appendix A

The value of adiabatic index in terms of Krori–Barua solution takes the form

$$\Gamma = -\Big[3\left\{Ar^2\left(4\varrho\mathfrak{B}_c\left(Br^2+2\right)+1\right)\right.$$
$$\left.-2\mathfrak{B}_c\left(\varrho+e^{Ar^2}\left(8\pi r^2-\varrho\right)\right)+Br^2\times(1-8\varrho\mathfrak{B}_c)\right\}\Big]^{-1}$$
$$\times[2r^2\left\{\varrho A^2\mathfrak{B}_c r^2+A\left(\varrho\mathfrak{B}_c\left(2Br^2+5\right)-2\right)\right.$$
$$\left.-B\left(2+\varrho\mathfrak{B}_c\times\left(1+3Br^2\right)\right)\right\}].$$

The term $|v_{s\perp}^2 - v_{sr}^2|$ in modified gravity becomes

$$|v_{s\perp}^2 - v_{sr}^2|$$
$$= \frac{1}{12}\Big|\Big[\left(\varrho\left(-Ar^2\left(Br^2+2\right)+B^2r^4+3Br^2+1\right)\right.$$
$$\left.+e^{Ar^2}\left(r^2-\varrho\right)\right)^2$$
$$\times\left\{\varrho A^3r^4\left(8\varrho\mathfrak{B}_c+2\mathfrak{B}_c e^{Ar^2}\left(r^2-\varrho\right)+1\right)\right.$$
$$+A^2r^2\left(e^{Ar^2}\left(2\varrho(2-3\varrho\mathfrak{B}_c)\right.\right.$$
$$\left.+4\varrho\mathfrak{B}_c Br^4-4r^2\left(-2\varrho\mathfrak{B}_c\right.\right.$$
$$\left.\left.+\varrho^2\mathfrak{B}_c B+1\right)\right)+\varrho\left(Br^2(11-12\varrho\mathfrak{B}_c)-4\varrho\mathfrak{B}_c\right)\Big)$$
$$+A\left(\varrho\left(-B^2\right)r^4\left(36\varrho\mathfrak{B}_c+6\mathfrak{B}_c e^{Ar^2}\left(r^2-\varrho\right)-7\right)\right.$$
$$-2Br^2\left(4\varrho^2\mathfrak{B}_c+e^{Ar^2}\left(r^2(3\varrho\mathfrak{B}_c+2)-\varrho(5\varrho\mathfrak{B}_c+2)\right)\right)$$
$$\left.+(5\varrho\mathfrak{B}_c-2)\left(e^{Ar^2}-1\right)2\varrho\right)$$
$$+\varrho B\left(2\varrho\mathfrak{B}_c+2e^{Ar^2}\left(-\varrho\mathfrak{B}_c+3\mathfrak{B}_c Br^2\left(r^2-2\varrho\right)-2\right)\right.$$
$$\left.\left.+3B^2r^4(8\varrho\mathfrak{B}_c-1)+12\varrho\mathfrak{B}_c Br^2+4\right)\right\}\Big]^{-1}$$
$$\times\Big[2\left(e^{Ar^2}\left(r^2-\varrho\right)+\left(B^2r^4\right.\right.$$
$$\left.+3Br^2-A\left(Br^2+2\right)r^2+1\right)\varrho\left)\left(4e^{Ar^2}\left(r^2-\varrho\right)\right.\right.$$
$$+\left(-A^2r^4+3B^2r^4+17Br^2-A\left(10Br^2+21\right)r^2+4\right)\varrho\Big)$$
$$\times\left\{r^2\varrho\left(3B(22\varrho\mathfrak{B}_c+1)r^2+88\varrho\mathfrak{B}_c\right.\right.$$
$$\left.-4e^{Ar^2}\left(3r^2+\varrho\right)\mathfrak{B}_c+14\right)A^3$$
$$+\left(\varrho\left(3B^2(10\varrho\mathfrak{B}_c+9)r^4+2Br^2(31-36\varrho\mathfrak{B}_c)\right.\right.$$
$$\left.-8\varrho\mathfrak{B}_c+11\right)-4e^{Ar^2}\left(Br^4+(-B\varrho+5\mathfrak{B}_c\varrho+1)r^2\right.$$
$$\left.+\varrho(2\varrho\mathfrak{B}_c-1)\right)A^2+\left(4e^{Ar^2}\left(B^2\left(r^2-\varrho\right)(\varrho\mathfrak{B}_c+1)r^2\right.\right.$$
$$\left.-B\varrho+\varrho\mathfrak{B}_c-1\right)-B\varrho\left(39B^2(2\varrho\mathfrak{B}_c+1)r^4\right.$$
$$\left.+2B(64\varrho\mathfrak{B}_c+55)r^2+8\varrho\mathfrak{B}_c+69\right)\Big)A$$
$$+B\left(e^{Ar^2}\left(4B\left(2r^2-\varrho\right)(\varrho\mathfrak{B}_c+1)+8\right)\right.$$
$$+B\varrho\left(9B^2(6\varrho\mathfrak{B}_c+1)r^4+2B(28\varrho\mathfrak{B}_c+33)r^2\right.$$
$$\left.+6(\varrho\mathfrak{B}_c+7)\right)\Big)\Big\}r^2-2\left(e^{Ar^2}\left(A\left(r^2-\varrho\right)+1\right)\right.$$
$$+\left(B\left(2Br^2+3\right)-2A\left(Br^2+1\right)\right)\varrho\Big)\left(4e^{Ar^2}\left(r^2-\varrho\right)\right.$$
$$+\left(-A^2r^4+3B^2r^4+17Br^2-A\right.$$
$$\left.\times\left(10Br^2+21\right)r^2+4\right)\varrho\Big)$$
$$\times\left\{A^3\varrho\left(B(22\varrho\mathfrak{B}_c+1)r^2+44\varrho\mathfrak{B}_c+7\right)r^4\right.$$
$$+A^2\varrho\left(B^2(10\varrho\mathfrak{B}_c+9)r^4\right.$$
$$+B(31-36\varrho\mathfrak{B}_c)r^2-8\varrho\mathfrak{B}_c-4\left(3r^2+\varrho\right)$$
$$\times\mathfrak{B}_c e^{Ar^2}+11)r^2+B\left(4e^{Ar^2}\left(r^2-\varrho\right)\right.$$
$$\times\left(B(\varrho\mathfrak{B}_c+1)r^2+2\right)+\varrho\left(3B^3r^6\right.$$
$$\times(6\varrho\mathfrak{B}_c+1)+B^2(28\varrho\mathfrak{B}_c+33)r^4$$
$$\left.+6B(\varrho\mathfrak{B}_c+7)r^2+8\right))-A\left(4e^{Ar^2}\right.$$
$$\times\left(r^2-\varrho\right)\left(Br^2-\varrho\mathfrak{B}_c+1\right)$$
$$+\varrho\left(13B^3(2\varrho\mathfrak{B}_c+1)r^6+B^2(64\varrho\mathfrak{B}_c+55)r^4\right.$$
$$\left.\left.+B(8\varrho\mathfrak{B}_c+69)r^2-4\varrho\mathfrak{B}_c+4\right)\right)\Big\}r^2-2\left(e^{Ar^2}\left(r^2-\varrho\right)\right.$$
$$+\left(B^2r^4+3Br^2-A\left(Br^2+2\right)r^2+1\right)\varrho\Big)$$
$$\times\left(4e^{Ar^2}\left(A\left(r^2-\varrho\right)+1\right)+\left(-2A^2r^2+B\left(6Br^2+17\right)\right.\right.$$
$$\left.-A\left(20Br^2+21\right)\right)\varrho\Big)\Big\{A^3\varrho\left(B(22\varrho\mathfrak{B}_c+1)r^2+7\right.$$
$$\left.+44\varrho\mathfrak{B}_c\right)r^4+A^2\varrho\left(B^2(10\varrho\mathfrak{B}_c+9)r^4\right.$$
$$+B(31-36\varrho\mathfrak{B}_c)r^2-8\varrho\mathfrak{B}_c$$
$$-4e^{Ar^2}\left(3r^2+\varrho\right)\mathfrak{B}_c+11\Big)r^2$$
$$+B\left(4e^{Ar^2}\left(r^2-\varrho\right)\left(B(\varrho\mathfrak{B}_c+1)r^2+2\right)\right.$$
$$+\varrho\left(3B^3(6\varrho\mathfrak{B}_c+1)r^6+B^2(28\varrho\mathfrak{B}_c+33)r^4\right.$$
$$\left.+6B(\varrho\mathfrak{B}_c+7)r^2+8\right))$$
$$-A\left(4e^{Ar^2}\left(r^2-\varrho\right)\left(Br^2-\varrho\mathfrak{B}_c+1\right)\right.$$
$$+\varrho\left(13B^3(2\varrho\mathfrak{B}_c+1)r^6+B^2\right.$$
$$\times(64\varrho\mathfrak{B}_c+55)r^4+B(8\varrho\mathfrak{B}_c+69)r^2$$
$$\left.-4\varrho\mathfrak{B}_c+4\right)\Big)\Big\}r^2+2\left(e^{Ar^2}\left(r^2-\varrho\right)\right.$$
$$+\left(B^2r^4+3Br^2-A\left(Br^2+2\right)r^2+1\right)\varrho\Big)\left(4e^{Ar^2}\left(r^2-\varrho\right)\right.$$
$$+\left(4-A^2r^4+3B^2r^4+17Br^2-A\left(10Br^2+21\right)r^2\right)\varrho\Big)$$
$$\left\{A^3\varrho\left(B(22\varrho\mathfrak{B}_c+1)\right.\right.$$
$$\times r^2+44\varrho\mathfrak{B}_c+7\Big)r^4+A^2\varrho\left(B^2(10\varrho\mathfrak{B}_c+9)r^4\right.$$
$$+B(31-36\varrho\mathfrak{B}_c)r^2-8\varrho\mathfrak{B}_c$$
$$-4e^{Ar^2}\left(3r^2+\varrho\right)\mathfrak{B}_c+11\Big)r^2$$
$$+B\left(4e^{Ar^2}\left(r^2-\varrho\right)\left(B(\varrho\mathfrak{B}_c+1)r^2+2\right)\right.$$
$$+\varrho\left(3B^3(6\varrho\mathfrak{B}_c+1)r^6+B^2(28\varrho\mathfrak{B}_c+33)r^4\right.$$
$$\left.+6B(\varrho\mathfrak{B}_c+7)r^2+8\right))$$
$$-A\left(4e^{Ar^2}\left(r^2-\varrho\right)\left(Br^2-\varrho\mathfrak{B}_c+1\right)\right.$$
$$+\varrho\left(13B^3(2\varrho\mathfrak{B}_c+1)r^6+B^2(64\varrho\mathfrak{B}_c+55)r^4\right.$$
$$\left.\left.\left.+B(8\varrho\mathfrak{B}_c+69)r^2-4\varrho\mathfrak{B}_c+4\right)\right)\right\}-4\Big]\Big|.$$

References

[1] S Nojiri and S D Odintsov, *Phys. Rev. D* **68**, 123512 (2003)
[2] G Cognola, E Elizalde, S Nojiri, S D Odintsov and S Zerbini, *J. Cosmol. Astropart. Phys.* **2005**, 010 (2005)
[3] Y S Song, W Hu and I Sawicki, *Phys. Rev. D* **75**, 044004 (2007)
[4] S Capozziello, M De Laurentis, S D Odintsov and A Stabile, *Phys. Rev. D* **83**, 064004 (2011)
[5] M Sharif and H R Kausar, *J. Cosmol. Astropart. Phys.* **2011**, 022 (2011)
[6] S Arapoğlu, C Deliduman and K Y Ekşi, *J. Cosmol. Astropart. Phys.* **2011**, 020 (2011)
[7] R Goswami, A M Nzioki, S D Maharaj and S G Ghosh, *Phys. Rev. D* **90**, 084011 (2014)
[8] M Sharif and Z Yousaf, *Astropart. Phys.* **56**, 19 (2014)
[9] A V Astashenok, S Capozziello and S D Odintsov, *Phys. Rev. D* **89**, 103509 (2014)
[10] O Bertolami, C G Boehmer, T Harko and F S N Lobo, *Phys. Rev. D* **75**, 104016 (2007)
[11] T Harko, F S N Lobo, S Nojiri and S D Odintsov, *Phys. Rev. D* **84**, 024020 (2011)
[12] M Sharif and M Zubair, *J. Cosmol. Astropart. Phys.* **2012**, 028 (2012)
[13] H Shabani and M Farhoudi, *Phys. Rev. D* **88**, 044048 (2013)
[14] P H R S Moraes, J D V Arbañil and M Malheiro, *J. Cosmol. Astropart. Phys.* **2016**, 005 (2016)
[15] M Sharif and A Siddiqa, *Eur. Phys. J. Plus* **132**, 1 (2017)
[16] A Das, S Ghosh, B K Guha, S Das, F Rahaman and S Ray, *Phys. Rev. D* **95**, 124011 (2017)
[17] Z Haghani, T Harko, F S N Lobo, H R Sepangi and S Shahidi, *Phys. Rev. D* **88**, 044023 (2013)
[18] M Sharif and M Zubair, *J. High Energy Phys.* **2013**, 79 (2013)
[19] M Sharif and M Zubair, *J. Cosmol. Astropart. Phys.* **2013**, 042 (2013)
[20] S D Odintsov and D Sáez-Gómez, *Phys. Lett. B* **725**, 437 (2013)
[21] I Ayuso, J B Jiménez and A De la Cruz-Dombriz, *Phys. Rev. D* **91**, 104003 (2015)
[22] E H Baffou, M J S Houndjo and J Tosssa, *Astrophys. Space Sci.* **361**, 376 (2016)
[23] M Sharif and A Waseem, *Eur. Phys. J. Plus* **131**, 1 (2016)
[24] M Sharif and A Waseem, *Can. J. Phys.* **94**, 1024 (2016)
[25] Z Yousaf, M Z Bhatti and T Naseer, *Eur. Phys. J. Plus* **135**, 353 (2020)
[26] Z Yousaf, M Z Bhatti and T Naseer, *Phys. Dark Universe* **28**, 100535 (2020)
[27] Z Yousaf, M Z Bhatti and T Naseer, *Int. J. Mod. Phys. D* **29**, 2050061 (2020)
[28] Z Yousaf, M Z Bhatti and T Naseer, *Ann. Phys.* **420**, 168267 (2020)
[29] Z Yousaf, M Z Bhatti, T Naseer and I Ahmad, *Phys. Dark Universe* **29**, 100581 (2020)
[30] Z Yousaf, M Y Khlopov, M Z Bhatti and T Naseer, *Mon. Not. R. Astron. Soc.* **495**, 4334 (2020)
[31] M Sharif and T Naseer, *Chin. J. Phys.* **73**, 179 (2021)
[32] T Naseer and M Sharif, *Universe* **8**, 62 (2022)
[33] E Witten, *Phys. Rev. D* **30**, 272 (1984)
[34] A R Bodmer, *Phys. Rev. D* **4**, 1601 (1971)
[35] I Bombaci, *Phys. Rev. C* **55**, 1587 (1997)
[36] L Herrera, *Phys. Lett. A* **165**, 206 (1992)
[37] L Herrera and N O Santos, *Phys. Rep.* **286**, 53 (1997)
[38] T Harko and M K Mak, *Ann. Phys.* **11**, 3 (2002)
[39] S K M Hossein, F Rahaman, J Naskar, M Kalam and S Ray, *Int. J. Mod. Phys. D* **21**, 1250088 (2012)
[40] M Kalam, F Rahaman, S Molla and S K M Hossein, *Astrophys. Space Sci.* **349**, 865 (2014)
[41] B C Paul and R Deb, *Astrophys. Space Sci.* **354**, 421 (2014)
[42] G H Bordbar and A R Peivand, *Res. Astron. Astrophys.* **11**, 851 (2011)
[43] P Haensel, J L Zdunik and R Schaefer, *Astron. Astrophys.* **160**, 121 (1986)
[44] K S Cheng, Z G Dai and T Lu, *Int. J. Mod. Phys. D* **7**, 139 (1998)
[45] P B Demorest, T Pennucci, S M Ransom, M S E Roberts and J W T Hessels, *Nature* **467**, 1081 (2010)
[46] F Rahaman, K Chakraborty, P K F Kuhfittig, G C Shit and M Rahman, *Eur. Phys. J. C* **74**, 1 (2014)
[47] P Bhar, *Astrophys. Space Sci.* **357**, 1 (2015)
[48] J D V Arbañil and M Malheiro, *AIP Conf. Proc.* **1693**, 030007 (2015)
[49] D Deb, S R Chowdhury, S Ray, F Rahaman and B K Guha, *Ann. Phys.* **387**, 239 (2017)
[50] D Deb, M Khlopov, F Rahaman, S Ray and B K Guha, *Eur. Phys. J. C* **78**, 465 (2018)
[51] M Sharif and A Waseem, *Eur. Phys. J. C* **78**, 868 (2018)
[52] M Sharif and A Waseem, *Int. J. Mod. Phys. D* **28**, 1950033 (2019)
[53] M Sharif and A Waseem, *Chin. J. Phys.* **63**, 92 (2020)
[54] M Sharif and A Majid, *Eur. Phys. J. Plus* **135**, 1 (2020)
[55] M Sharif and A Majid, *Universe* **6**, 124 (2020)
[56] M Sharif and A Majid, *Astrophys. Space Sci.* **366**, 1 (2021)
[57] N K Glendenning, *Phys. Rev. D* **46**, 1274 (1992)
[58] M Kalam, A A Usmani, F Rahaman, S M Hossein, I Karar and R Sharma, *Int. J. Theor. Phys.* **52**, 3319 (2013)
[59] J D V Arbañil and M Malheiro, *J. Cosmol. Astropart. Phys.* **2016**, 012 (2016)
[60] K D Krori and J Barua, *J. Phys. A: Math. Gen.* **8**, 508 (1975)
[61] K Lake, *Phys. Rev. D* **67**, 104015 (2003)
[62] M Dey, I Bombaci, J Dey, S Ray and B C Samanta, *Phys. Lett. B* **438**, 123 (1998)
[63] X D Li, I Bombaci, M Dey, J Dey and E P J Van Den Heuvel, *Phys. Rev. Lett.* **83**, 3776 (1999)
[64] H A Buchdahl, *Phys. Rev.* **116**, 1027 (1959)
[65] B V Ivanov, *Phys. Rev. D* **65**, 104011 (2002)
[66] H Heintzmann and W Hillebrandt, *Astron. Astrophys.* **38**, 51 (1975)